Computational Study of Structures and Properties of Metallaboranes: Cobalt Bis(dicarbollide)

Michael Bühl,*[a] Drahomír Hnyk,[b] and Jan Macháček[b]

Dedicated to Professor Paul von Ragué Schleyer on the occasion of his 75th birthday

Abstract: A density functional study at the BP86/AE1 level is presented for the cobalt bis(dicarbollide) ion [3-Co-(1,2-$C_2B_9H_{11}$)$_2$]$^-$ (**1**) and selected isomers and rotamers thereof. Rotation of the two dicarbollide moieties with respect to each other is facile, as judged by the small energetic separation of the three rotamers located (within 11 kJ mol^{-1}) and by the low barriers for their interconversion (at most 41 kJ mol^{-1}). Among the isomers differing in carbon atom positions that contain two equivalent dicarbollide ligands, the 1,7 ("carbon apart") form [2-Co-(1,7-$C_2B_9H_{11}$)$_2$]$^-$ is the most stable, 121 kJ mol^{-1} below **1**. The electronic structure of **1** is characterized in terms of molecular orbitals, population analysis, and excitation energies from time-dependent density functional theory, relevant to UV/Vis spectroscopy. Experimental ^{11}B NMR chemical shifts of **1** are reproduced to better than 5 ppm at the GIAO-B3LYP/II′ level, and the computed $\delta(^{11}B)$ values are only little affected by rotational averaging or the presence of a polarizable continuum. Larger such effects are found for the as-yet unknown ^{59}Co chemical shift, for which a value in the range between −1800 and −2400 ppm is predicted. Even though the accuracy achieved for the theoretical $\delta(^{11}B)$ values is somewhat lower than that for heteroboranes at conventional ab initio levels, the level of density functional employed can afford qualitatively reliable chemical shifts, which can be useful in assignments and structural refinements of heteroboranes containing transition metal.

Keywords: carboranes · cobalt · density functional calculations · NMR spectroscopy

Introduction

The chemistry of polyhedral boron compounds, potentially as extensive and rich as the organic chemistry of carbon, provides an important bridge between well-behaved organic molecules and the chemistry of metals, which is still insufficiently understood. In boron hydrides, which stand out due to their unique architecture, chemical bonding, and physical properties, the boron atoms can be substituted by almost any element affording heteroboranes such as carbaboranes (or carboranes) and metallaboranes. Even though a plethora of such derivatives are known, these constitute just a small fraction of theoretically possible compounds. The unique properties of these compounds and the possibility of their systematic variation by substitution of skeletal B atoms (besides that of exohedral H atoms) make them an important and very attractive class of materials.

A major part of the huge area of deltahedral compounds comprises the metallaheteroborane clusters, most prominent among which are the *commo*-bis(icosahedral)metallacarbaboranes of the type [M(C$_2$B$_9$H$_{11}$)$_2$]$^{n-}$.[1–3] Each family can contain as many as 48 isomers (including diastereomers) differing in mutual arrangements of the carbon atoms. Of these just two isomers are known: one with adjacent, the other with nonadjacent carbon vertices.[2] There are over ten families with different central metal atoms sandwiched between two deltahedral eleven-vertex ligands.

The most investigated and best known is the [3-Co-(1,2-C$_2$B$_9$H$_{11}$)$_2$]$^-$ ion, mostly referred to as the cobalt bis(dicarbollide) ion (**1**, see Figure 1).[3] This species can be considered as an archetype of all metallaheteroboranes. Hundreds

[a] Dr. M. Bühl
Max-Planck-Institut für Kohlenforschung
Kaiser-Wilhelm-Platz 1
45470 Mülheim/Ruhr (Germany)
Fax: (+49) 208-306-2996
E-mail: buehl@mpi-muelheim.mpg.de

[b] Dr. D. Hnyk, J. Macháček
Institute of Inorganic Chemistry
Czech Academy of Sciences, Řež near Prage (Czech Republic)

Supporting information for this article is available on the WWW under http://www.chemeurj.org/ or from the author.

 DOI: 10.1002/chem.200401202

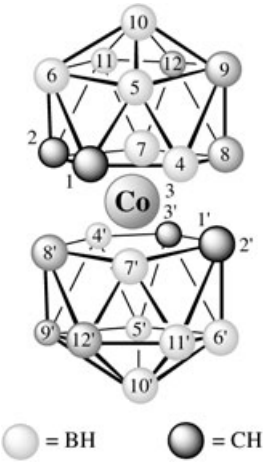

Figure 1. Skeletal structure and numbering scheme of $[Co(C_2B_9H_{11})_2]^-$; B and C atoms in light and dark gray, respectively, H atoms not shown.

of derivatives were prepared and dozens of X-ray structures have been established.[4] Essentially all species of this kind have been characterized by multinuclear NMR spectroscopy. However, no modern computational analysis even of the parent archetype ion has been reported.[5] This situation is rather deplorable, because several derivatives of **1** became the most prominent solvent extraction agents for separation and isolation of fission radionuclides from nuclear waste, which is their only application on an engineering scale so far.[6] Other species of this kind have been suggested for modification of various plastics to obtain selective color filters, ferroelectric composites, potential devices showing nonlinear optical phenomena, and so on.

We now report a computational study on this prototypical metallacarborane, with special attention to energetics of its isomers and conformers, as well as their NMR chemical shifts. In particular, ^{11}B NMR spectroscopy is one of the principal means of characterization for boron-based compounds. The combination of observed and theoretically calculated $\delta(^{11}B)$ values has been developed into a structural tool for boranes and heteroboranes.[7–9] The methodology established for these classes of compounds, that is, optimization of geometries at correlated ab initio levels and chemical shift computations at IGLO-SCF, GIAO-SCF, or GIAO-MP2 levels, is being routinely applied as an independent tool for characterization of newly synthesized borane and carbaborane derivatives,[9] and the credibility of structural assigments based on this method has been attested to "rival that of X-ray crystallography".[10]

These assignments rely on an accuracy of about 2–3 ppm that can be achieved for the computed ^{11}B chemical shifts. To approach similar accuracy for molecules containing transition-metal atoms, it may be necessary to go beyond these low ab initio levels (Hartree–Fock or MP2) in the chemical-shift computation. Even though, in some favorable cases, ^{11}B and even the more demanding transition-metal chemical shifts themselves have been reproduced reasonably well at such levels,[11] the modern tools of density functional theory (DFT) are now the established method of choice for this kind of substances.[12–14] The impressive performance for $\delta(^{13}C)$, $\delta(^{17}O)$, and $\delta(^{1}H)$ of ligands in the coordination sphere of transition metals was one of the early successes of DFT-based approaches for chemical-shift calculations.[12] We now test the applicability of these tools to metallacarboranes such as **1**. As it turns out, DFT methods can pass this test, and this has important implications for their future application to this class of compounds.

Computational and Experimental Details

Stationary points were optimized at the BP86/AE1 level, that is, by employing the exchange and correlation functionals of Becke[15] and Perdew,[16] respectively, together with a fine integration grid (75 radial shells with 302 angular points per shell) and an all-electron basis consisting of the augmented Wachters' basis[17] on Co (8s7p4d, full contraction scheme 62111111/3311111/3111) and 6-31G* basis on all other elements.[18] This and comparable DFT levels have proven quite successful for transition-metal compounds and are well suited for the description of structures, energies, barriers, and so on.[19] The nature of the stationary points was verified by computations of the harmonic frequencies at that level. Transition states were characterized by a single imaginary frequency, and visualization of the corresponding vibrational modes ensured that the desired minima are connected. Unless otherwise noted, energies are reported at the BP86/AE1 level. Zero-point corrections afforded only minor changes in relative energies: less than 1 kJ mol^{-1} for minima and less than 2 kJ mol^{-1} for transition states. Natural population analysis[20] and topological analysis of the total electron density[21] were performed at the BP86/AE1 level. Optimized coordinates of each isomer (single rotamer only) are provided as Supporting Information.

Magnetic shieldings were computed for BP86/AE1 geometries by employing gauge-including atomic orbitals (GIAOs),[22] the B3LYP[23,24] hybrid functional, together with basis II′, which consists of the same Wachters' basis set on Co as described above, a contracted (5s4p1d) Huzinaga basis of polarized triple-zeta quality on C and B, and a double-zeta basis (2s) on H.[25] This particular combination of density functionals and basis sets has proven to perform well for the computation of transition-metal chemical shifts.[13a] With the same combination of functional and basis set, excitation energies and oscillator strengths have been computed with time-dependent density functional theory (TDDFT).[26]

^{13}C chemical shifts are reported relative to TMS, computed at the same level (C shielding constant 181.1 ppm). ^{11}B chemical shifts were calculated relative to B_2H_6 (B shielding constant 81.4 ppm) and converted to the usual $BF_3{\cdot}OEt_2$ scale by using the experimental $\delta(^{11}B)$ value of B_2H_6 of 16.6 ppm.[27] Likewise, ^{59}Co chemical shifts were calculated relative to the cobalticenium ion $[Co(C_5H_5)_2]^+$ (Co shielding constant −3089 ppm) and converted to the usual aqueous $K_3[Co(CN)_6]$ reference by using the experimental $\delta(^{59}Co)$ value of $[Co(C_5H_5)_2]^+$ of −2410 ppm.[28]

In some exploratory calculations, other functionals were also tested: LDA (in the SVWN5 implementation in Gaussian),[29] PBE,[30] and BHLYP (with Becke's half-and-half exchange part).[31] All computations were performed with the Gaussian 03 program,[32] except for the topological analysis, which was performed with Morphy.[33]

^{11}B and ^{13}C NMR spectra of Cs[3-Co-(1,2-$C_2B_9H_{11})_2$] and Cs[2-Co-(1,7-$C_2B_9H_{11})_2$] in CD_3CN solution were measured in Řež on a Varian Mercury Plus 400 NMR spectrometer under standard conditions on samples kindly provided by J. Plešek and J. Bačkovský. ^{13}C chemical shifts are given relative to TMS with the nitrile signal of the deuterated lock solvent (at $\delta = 118.2$ ppm) as internal reference; ^{11}B chemical shifts are given relative to $BF_3{\cdot}OEt_2$ and referenced to $(CH_3O)_3B$ (at $\delta = 18.1$ ppm) as external standard.

Table 1. BP86/AE1 optimized geometrical parameters [Å, °] for **1** and its rotamers. In italics: experimental X-ray values, where available.

θ_{ideal}[a]	θ[a]	Co–C1	Co–C2	Co–B4	Co–B7	Co–B8	C1–C2	C1–B4
180	180.0	2.027	2.027	2.112	2.112	2.160	1.639	1.721
Exptl[b]	*180.0*	*2.024*	*2.017*	*2.111*	*2.082*	*2.141*	*1.632*	*1.708*
Exptl[c]	*180.0*	*2.136*	*2.097*	*2.125*	*2.115*	*2.184*	*1.574*	*1.706*
108	114.1	2.029	2.049	2.092	2.117	2.146	1.631	1.724
Exptl[d]	*110.6*	*2.063/2.028*	*2.061/2.031*	*2.061/2.116*	*2.067/2.169*	*2.063/2.083*	*1.622/1.582*	*1.701/1.633*
36	41.2	2.045	2.052	2.094	2.108	2.131	1.627	1.721
Exptl[e]	*37.9*	*2.042/2.058*	*2.038/2.041*	*2.098/2.099*	*2.090/2.078*	*2.109/2.102*	*1.625/1.621*	*1.709/1.686*
144	146.8	2.039	2.051	2.120	2.129	2.171	1.628	1.715
72	75.0	2.053	2.067	2.108	2.130	2.161	1.622	1.720
0	0.0	2.070	2.070	2.122	2.122	2.147	1.619	1.712

θ_{ideal}	C1–B5	C1–B6	C2–B6	C2–B7	C2–B11	B4–B5	B4–B8	B4–B9
180	1.707	1.726	1.726	1.721	1.707	1.796	1.792	1.787
Exptl[b]	*1.697*	*1.714*	*1.729*	*1.717*	*1.704*	*1.776*	*1.786*	*1.776*
Exptl[c]	*1.694*	*1.726*	*1.747*	*1.712*	*1.703*	*1.805*	*1.774*	*1.789*
108	1.701	1.733	1.722	1.705	1.706	1.806	1.808	1.796
Exptl[d]	1.701/1.726	*1.694/1.747*	*1.689/1.679*	*1.706/1.709*	*1.690/1.679*	*1.798/1.848*	*1.803/1.824*	*1.803/1.772*
36	1.696	1.734	1.727	1.713	1.702	1.812	1.811	1.790
Exptl[e]	1.709/1.687	*1.744/1.707*	*1.737/1.720*	*1.697/1.699*	*1.695/1.673*	*1.790/1.793*	*1.785/1.766*	*1.762/1.771*
144	1.706	1.736	1.725	1.710	1.708	1.801	1.801	1.793
72	1.700	1.738	1.726	1.706	1.707	1.812	1.806	1.793
0	1.701	1.733	1.733	1.712	1.701	1.810	1.808	1.787

θ_{ideal}	B5–B6	B5–B9	B5–B10	B6–B10	B6–B11	B7–B8	B7–B11	B7–B12
180	1.773	1.781	1.785	1.775	1.773	1.792	1.796	1.787
Exptl[b]	*1.765*	*1.775*	*1.773*	*1.769*	*1.778*	*1.775*	*1.783*	*1.779*
Exptl[c]	*1.756*	*1.778*	*1.777*	*1.755*	*1.766*	*1.766*	*1.794*	*1.789*
108	1.772	1.784	1.784	1.776	1.769	1.798	1.797	1.782
Exptl[d]	*1.804/1.783*	*1.809/1.871*	*1.807/1.798*	*1.801/1.803*	*1.802/1.744*	*1.815/1.809*	*1.798/1.758*	*1.811/1.742*
36	1.769	1.784	1.783	1.775	1.769	1.809	1.804	1.780
Exptl[e]	*1.758/1.767*	*1.758/1.777*	*1.769/1.793*	*1.754/1.791*	*1.739/1.763*	*1.827/1.816*	*1.788/1.808*	*1.799/1.783*
144	1.768	1.783	1.784	1.774	1.769	1.792	1.798	1.786
72	1.768	1.780	1.783	1.772	1.769	1.801	1.802	1.781
0	1.766	1.779	1.782	1.772	1.766	1.808	1.810	1.787

θ_{ideal}	B8–B9	B8–B12	B9–B10	B9–B12	B10–B11	B10–B12	B11–B12
180	1.796	1.796	1.789	1.788	1.785	1.789	1.781
Exptl[b]	*1.781*	*1.786*	*1.788*	*1.774*	*1.786*	*1.787*	*1.777*
Exptl[c]	*1.785*	*1.785*	*1.783*	*1.769*	*1.776*	*1.781*	*1.773*
108	1.794	1.804	1.791	1.791	1.784	1.789	1.779
Exptl[d]	*1.806/1.839*	*1.806/1.856*	*1.808/1.898*	*1.811/1.788*	*1.807/1.825*	*1.802/1.838*	*1.810/1.786*
36	1.802	1.811	1.790	1.794	1.783	1.791	1.781
Exptl[e]	*1.810/1.786*	*1.818/1.794*	*1.770/1.787*	*1.784/1.773*	*1.767/1.762*	*1.779/1.776*	*1.792/1.769*
144	1.796	1.802	1.789	1.787	1.783	1.790	1.779
72	1.800	1.810	1.788	1.788	1.783	1.790	1.777
0	1.811	1.811	1.789	1.788	1.782	1.789	1.779

[a] θ: dihedral angle B8′-Co-B10-B8; θ_{ideal}: idealized value (see text). [b] QAJNAQ (as in H-relaxed geometry); experimental geometries from reference [4]. [c] RINMIK. [d] WEZHOY. [e] BEVBUZ.

Results and Discussion

Throughout this paper, individual isomers are designated by the positions of the carbon atoms, whereby we have adopted the single numbering scheme depicted in Figure 1, which is the commonly accepted one for the 1,2-isomer shown. Only symmetrical isomers with two equivalent dicarbollide moieties are considered; most of these have a C_2 axis, so that the

label *x*,*y* denotes an isomer with carbon atoms shifted from positions 1,2,1′,2′ to *x*,*y*,*x*′,*y*′. When each dicarbollide unit is chiral, not only the symmetrical C_2 form was considered (designated as *x*,*y*s), but also its diastereomer with one dicarbollide unit changed to its mirror image (denoted *x*,*y*a). Rotamers are identified by a suitable dihedral angle given in the text.

Geometries and energies: A number of solids containing **1** and various counterions and cocrystallized molecules have been analyzed by X-ray crystallography.[4] In the majority of cases, the metallaborane adopts the *trans* conformation depicted in Figure 1 with exact or idealized C_{2h} symmetry. At the BP86/AE1 level, the pristine anion is indeed a minimum in this symmetry. Salient optimized geometrical parameters are collected in Table 1 and are compared to selected experimental data. Overall, the optimized bond lengths reproduce the solid-state data fairly well, usually within a few picometers, a degree of agreement which is typical for the DFT level employed.[19] Note that the experimental values can vary substantially from one crystal to another (e.g., compare the two sets of experimental data for $\theta = 180°$ in Table 1), or from one dicarbollide unit to the other if they are inequivalent due to lower symmetry in the crystal.

Occasionally, **1** adopts different conformations in the solid state, in which the two carborane moieties are rotated with respect to each other along the axis passing through B10 and B10′. As a measure for this rotation, we use the B8-Co3-B10-B8 dihedral angle θ, which is 180° for C_{2h}-symmetric **1**. The other rotamers observed are characterized by $\theta =$ 110.6 and 37.9°, values which are close to the idealized angles for rotation about a fivefold axis (108 and 36°, respectively) and are reasonably well reproduced in the BP86 minima ($\theta = 114.1$ and 42.1°, respectively). As expected, the bond lengths are very similar for all three rotamers (see Table 1).

Relative energies of these rotamers are collected in Table 2 (see entry 1,2 with label **1**). The minima at $\theta = 180°$ and $\theta \approx 108°$ are very similar in energy, and the rotamer with $\theta \approx 36°$ is slightly less stable, by about 10 kJ mol^{-1}. These results are consistent with the observation that more than one conformation can be found in the same crystal.[4a] We also studied the full rotational profile by locating all transition states along this path. As expected, transition states are found at θ values around 0, 72, and 144° (see Table 1 for the exact values), where the two C_2B_3 rings connected to the metal atom are in an eclipsed conformation. In these conformations, the Co–C and Co–B distances are somewhat elongated with respect to the corresponding ones in the staggered minima (Table 1). The main factor contributing to this destabilizing effect is probably mutual repulsion of the hydrogen atoms attached to the two C_2B_3 rings (not shown in Figure 1), which approach each other to about 2.2–2.3 Å in the transition structures (2.5–2.7 Å in the minima). This repulsion is absent in the related cobalticenium cation $[Co(C_5H_5)_2]^+$ due to the much larger Co-X-H angles than in the metallacarborane, and this ferrocene analogue adopts an eclipsed equilibrium conformation.[34]

The computed rotational barriers, relative to the lowest minimum, are between about 15 and 37 kJ mol^{-1} (see entries

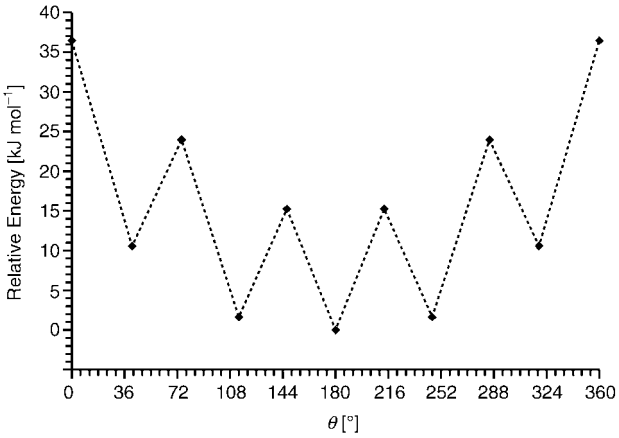

Figure 2. Schematic energy profile for rotation about the B10–B10′ axis in **1** (BP86/AE1 level; θ: 8′-3-10-8 dihedral angle).

Table 2. Relative energies [kJ mol^{-1}] of **1** ($E_{rel} = 0$) and selected isomers and rotamers (BP86/AE1 level).

Isomer[a]	θ[b]|θ_{ideal}:	180°	108°	36°	144°	72°	0°
5,10 (9,1,2)	B7′-Co-B10-B7	102.2	102.9	104.9	119.6	120.5	122.0
5,6 (8,1,2)	B1′-Co-B10-B1	68.9	70.5	73.7	84.9	88.5	91.1
1,5s (4,1,2)	C1′-Co-B10-C1	35.8	42.4	45.0	56.8	60.3	68.5
1,5a (4,1,2)	C1′-Co-B10-C1	34.9	39.0	43.3	53.5	56.9	70.1
1,2 (3,1,2) **1**	B8′-Co-B10-B8	0.0	1.6	10.6	15.2	24.0	36.5
1,10 (2,1,9)	C1′-Co-C10-C1	−50.9	−50.4	−49.4	−30.7	−34.1	−23.4
5,11 (9,1,7)	B8′-Co-B10-B8	−54.3	−52.2	−52.1	−37.0	−36.3	−35.0
1,9s (2,1,8)	C1′-Co-B10-C1	−81.4	−80.9	−81.1	−61.4	−67.0	−62.0
1,9a (2,1,8)	C1′-Co-B10-C1	−83.1	−85.2	−83.2	−66.8	−71.6	−59.6
1,12 (2,1,12)	C1′-Co-B10-C1	−100.7	−101.7	−105.8	−81.7	−90.7	−82.8
1,7 (2,1,7)	B2′-Co-B10-B2	−111.7	−120.6	−118.0	−92.0	−110.1	−77.0

[a] Isomers labeled according to the numbering in Figure 1; in parentheses: official numbering scheme in which one C atom is assigned position 1 (number in the middle), and the other C and Co atoms, which are denoted by the third and first number, respectively, are given the lowest possible values in a spiral counting scheme. [b] Definition of rotation angle; idealized values with 180, 108, and 36° denote minima, those with 144, 72, and 0° denote transition states (see text).

with $\theta \approx 144°$, 72°, and 0° for **1** in Table 2, and Figure 2 for a plot); the highest value occurs for the C_{2v}-symmetric form with $\theta = 0°$. In this rotamer, another destabilizing effect comes to the fore, namely, electrostatic repulsion of the C and B atoms with their respective like partial charges. Even with this highest barrier, rotation is quite facile at ambient temperature, and is essentially unhindered on the NMR timescale.

Isomerism is not as frequently encountered in borane

chemistry as in the organic chemistry of carbon compounds, because barriers between isomers tend to be lower in the former case than in the latter. Thus, boranes and heteroboranes are often isolated solely in form of the corresponding global minima. Icosahedral heteroboranes are notable exceptions, and the most prominent examples are the well-known *ortho*-, *meta*-, and *para*-carboranes $C_2B_{10}H_{12}$. Isomers are also known for the title compound, formally a derivative of *ortho*-carborane. The 1,7- (or "carbons-apart") form has been characterized spectroscopically,[35] and exohedrally substituted variants thereof also by X-ray crystallography.[36] In conjunction with other coligands, essentially all isomeric $[Co(C_2B_9)]$ cores have been realized;[37,38] in some cases they arose from skeletal rearrangement at elevated temperatures.[38,39]

We subsequently computed all symmetric ($x,y,x'y'$) isomers that contain a pair of equivalent carborane moieties (in total eleven forms, out of the much larger number of possible isomers that include nonequivalent ligands), as well as their rotamers and the corresponding transition states. The resulting rotational profiles of these isomers, assessed by suitable B′-Co-B10-B dihedral angles, show similar characteristics to that of the 1,2 parent, namely, three staggered minima separated by three eclipsed transition states (Table 2). The corresponding barriers (up to 41 kJ mol^{-1} for the 1,7 isomer) are all of the same order of magnitude as those in the 1,2 parent **1** and are low enough to allow facile rotation, which is again essentially free on the NMR timescale. The spread in relative energies between the isomers is much larger, covering more than 200 kJ mol^{-1} (Table 2). In this set, the 1,7 isomer is predicted to be the most stable and is likely to be the global minimum. The almost ubiquitous 1,2 isomer **1** is thus only metastable and its predominance is rooted in the way of its preparation, which uses the inexpensive *ortho*-carborane as starting material. Isomers with adjacent C atoms are the least stable (see first five entries in Table 2). This result is fully consistent with empirical stability rules, according to which heteroatoms prefer nonadjacent positions in deltahedral cages.[40] These rules have recently been quantified in terms of DFT-derived increment systems.[41]

Electronic structure: This section focuses on selected aspects of bonding and electron distribution in the title compound, with restriction to the C_{2h}-symmetric 1,2-isomer **1**. With formal Co^{III} (d^6) and $C_2B_9H_{11}^{2-}$ units, the latter being isolobal with $C_5H_5^-$, the bonding between metal and ligands in **1** resembles that in ferrocene to a large degree.[42] Highest occupied and lowest unoccupied Kohn–Sham MOs (Figure 3) exhibit the expected predominant d(metal) and pronounced ligand character, respectively.

Owing to the electronegativity difference between boron and carbon, the electrons are not equally distributed within the dicarbollide ligand, but are concentrated near the C atoms. This polarization of electron density is visible in the computed electrostatic potential (not shown), as well as in atomic charges, derived by using various definitions. Those

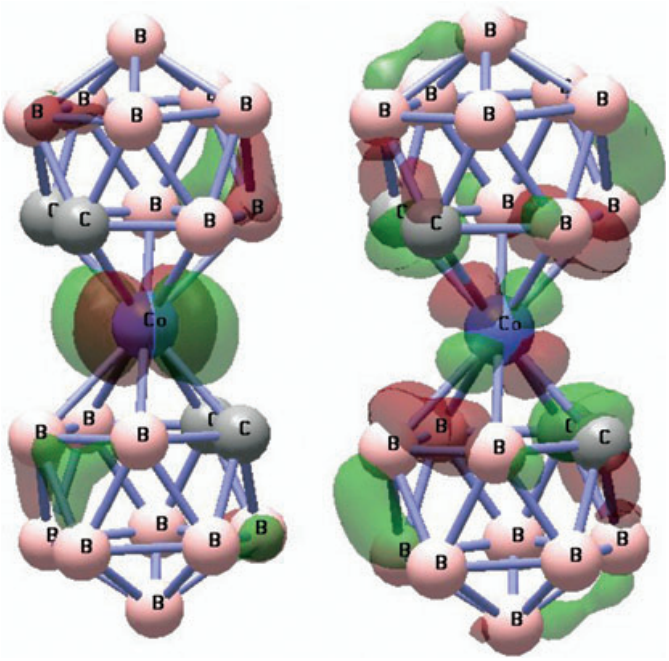

Figure 3. HOMO (left) and LUMO (right) of **1** (BP86/AE1 level).

Table 3. Atomic charges of **1** from natural population analysis (NPA).

Atom	q(NPA) BP86/AE1	q(NPA) B3LYP/II′
Co	0.21	0.32
C(1,2)	−0.52	−0.44
B(4,7)	−0.06	−0.05
B(8)	−0.23	−0.21
B(5,11)	−0.04	−0.11
B(6)	0.11	0.02
B(9,12)	−0.19	−0.23
B(10)	−0.18	−0.20

resulting from natural population analysis (NPA)[20] are collected in Table 3. As can be seen from the similarity of the BP86/AE1 and B3LYP/II′ data, the overall qualitative electron distribution is not overly sensitive to theoretical level and basis set.

Topological analysis[21] of the BP86/AE1 total electron density ρ reveals a bond path and a bond critical point (BCP) between the metal atom and each of the ten adjacent C and B atoms. The relatively low values of ρ and its Laplacian $\nabla^2\rho$ at these BCPs of 0.08–0.09 and 0.07–0.26 a.u., respectively, are indicative of notable ionic bonding, rather than predominantly shared (covalent) interactions. Similar results are obtained for the ferrocene-like cobalticenium cation. Bond indices according to Wiberg's definition,[43] a measure for covalent bonding, are about 0.19–0.25 between Co and C or B in **1**, consistent with pronounced ionic character.

The optical excitations of **1** were computed with time-dependent DFT, which has been shown to hold great promise for transition-metal complexes.[44] Since in many cases

hybrid functionals perform very well for low-lying electronic transitions,[26a] also for transition-metal compounds,[44b] we computed the excitation energies at the B3LYP level, employing the same basis (II′) as used in the NMR computations discussed below. As can be seen from the results summarized in Table 4, many transitions are computed in the visible region above 380 nm, consistent with the HOMO–LUMO gap (4.53 eV at B3LYP/II′) and close spacing of the Kohn–Sham MOs. All of these excitations, however, have zero computed intensity, and the lowest band with nonvanishing oscillator strength is no. 7 at 350 nm, which results essentially from the (HOMO−1)→LUMO transition (Table 4).

Table 4. Electronic transitions in **1** at the TDDFT/B3LYP/II′ level.

No.	Main contributions[a]	λ_{max} [nm][b]	Exptl[c,d]	Exptl[c,e]
1	80→83/82→84	542.1 (0.000)		
2	80→84/82→83	535.9 (0.000)		
3	80→84/75→84/82→83	458.2 (0.000)		
4	80→83	455.7 (0.000)	445 (440)	
5	75→84/76→84	360.8 (0.000)		
6	75→83/76→83	351.6 (0.000)		
7	81→83	349.6 (0.001)		
8	81→84/79→83	334.7 (0.015)	345 (2200)	
9	79→84	314.3 (0.006)		
10	77→84	275.8 (0.000)		
11	79→83/81→84	275.6 (0.559)	293 (45000)	287 (30980)
12	78→83	265.8 (0.008)		
14	78→84	265.0 (0.065)		
21	73→83/74→84	242.8 (0.001)		
22	73→84	242.4 (0.043)		
23	73→84	239.3 (0.007)		
27	69→84	229.9 (0.003)		
29	69→83	229.1 (0.027)		
31	70→84	227.1 (0.001)		
32	66→83	218.5 (0.002)		
34	66→84	213.9 (0.178)	216 (36300)	
40	81→85	194.4 (0.006)		

[a] Kohn–Sham MO numbers (HOMO: no. 82); only contributions larger than 0.3 are listed. [b] In parentheses: oscillator strengths in a.u. For states higher than no. 10, only those with nonzero oscillator strengths are given. [c] Cs^+ salt in methanol; in parentheses: ε_λ in $M^{-1}cm^{-1}$. [d] Reference [35]. [e] Reference [45].

The largest intensity is computed for band no. 11 in the near-UV at 277 nm, in very good agreement with the very strong absorption observed in the same region.[35,45] In terms of excitations from Kohn–Sham MOs, this band is mainly a transition from high-lying borane-skeleton bonding MOs into the LUMO/LUMO+1 pair. The shoulder observed[35] at 345 nm is also very well reproduced (see entry no. 8 in Table 4). The second strong absorption observed in the UV region at 219 nm[35] is also well reproduced (see entry no. 34 in Table 4) and is indicated to be essentially an excitation from a low-lying skeleton bonding MO (with large coefficients at the C atoms and the "antipodal" BH units at B10 and B10′) into the LUMO+1.

The orange color of solids and solutions containing the cobalt bis(dicarbollide) ion stems from an absorption at 445 nm,[35] which is very weak compared to these strong bands in the UV region. For C_{2h}-symmetric **1**, two bands are computed in the same region (entries no. 3 and 4 in Table 4), but both with zero intensity. Quite possibly, one or more of these transitions becomes allowed when the symmetry is reduced, for instance, in vibrating **1** or in the C_2-symmetric rotamers, which may be populated under experimental conditions. In fact, for the rotamer with $\theta \approx 36°$, a band at $\lambda_{max} = 451$ nm with a small but nonzero rotational strength (0.001 a.u.) is computed, in very good agreement with experiment. Thus, the salient features of the UV/Vis spectrum of **1** are well reproduced by TDDFT at the B3LYP level, and this allow for the theoretical interpretation of this spectrum and, presumably, those of other members of the large family of metal carbollide complexes as well. Deviations from experiment can amount to 10–20 nm for **1** (0.1–0.2 eV), similar to or even slightly better than what has been achieved for other transition-metal complexes, for which errors of several tenths of an electron volt are common.[44c]

Chemical shifts: Chemical shifts of **1** and of selected isomers and rotamers are summarized in Table 5. For comparison, the $\delta(^{11}B)$ and $\delta(^{13}C)$ values of the three carboranes $C_2B_{10}H_{12}$ are given in Table 6.

^{11}B: When comparing the $\delta(^{11}B)$ data computed for pristine **1** ($\theta = 180°$) to the observed[46] values, it appears that most of them are systematically shifted to higher field (i.e., to lower frequency). The unweighted mean absolute deviation from experiment (Cs^+ salt) is 3.3 ppm, with a maximum error of 4.7 ppm for the B(5,11) signal (Table 5). Similar results are obtained for the metal-free carborane isomers,[47] for which the overall mean absolute and maximum errors are 2.4 and 4.1 ppm, respectively (Table 6). Somewhat better accuracy was obtained for smaller carboranes at suitable ab initio levels, with maximum deviations from experiment on the order of 3 ppm.[7a] It thus appears that the errors in the theoretical $\delta(^{11}B)$ values of **1** are due to inherent shortcomings of the DFT approach in describing the basic *closo*-carborane motif, rather than complications brought about by the presence of the transition metal.[48]

Since the deviations are rather systematic, the theoretical $\delta(^{11}B)$ values could be improved by using a different primary standard. For instance, if 1,12-$C_2B_{10}H_{12}$ were used instead of B_2H_6 (see Computational Details), all calculated ^{11}B data would be shifted to lower field by 2.3 ppm (the difference between calculated and experimental values for the 1,12-isomer in Table 6), which would lead to a noticeably better accord with experiment in the majority of cases.[49]

Even with such an adjustment, however, one problem would remain for the computed ^{11}B chemical shifts of **1**, namely, the large difference between the B(4,7) and B(9,12) resonances, which amounts to 5.6 ppm (see Table 5). Experimentally, in contrast, these signals are observed very close to each other and can even be, as in the Cs^+ salt in acetone,[46b] accidentally degenerate. To test whether this apparent inconsistency could arise from possible shortcomings in the underlying DFT geometry (sometimes small changes in geo-

Table 5. Chemical shifts [ppm] of **1** and selected rotamers and isomers (GIAO-B3LYP/II′//BP86/AE1 level).[a] In italics: Experimental data, where available.

Isomer	θ_{ideal}	Nuclei							
		B(8)	B(10)	B(4,7)	B(9,12)	B(5,11)	B(6)	C(1,2)	Co
1,2 (**1**)	180°	3.9	−2.4	−3.9	−9.5	−21.9	−26.0	61.1	−1843
	108°	7.8	−3.0	−6.2 (−8.0/−4.3)	−9.0 (−9.8/−8.1)	−21.3(−23.1/−19.4)	−27.8	61.6 (62.7/60.4)	−1918
	36°	8.8	−3.2	−5.6 (−6.1/−5.0)	−7.3 (−8.7/−5.8)	−22.1(−22.9/−21.3)	−28.5	60.1 (58.2/61.9)	−2042
Exptl[b]		*6.5*	*1.4*	*−6.0*	*−6.0*	*−17.2*	*−22.7*	*51.5*[c]	–
Exptl[c]		*5.8*	*0.9*	*−6.0*	*−6.6*	*−17.6*	*−23.0*	*51.9*	–
{*Exptl*[d]}		*5.6*	*1.7*	*−5.9*	*−5.9*	*−16.4*	*−22.2*		

		B(4,8)	B(10)	B(2)	B(9)	B(5,12)	B(6,11)	C(1,7)	Co
1,7	180°	−2.3	−2.8	−8.9	−15.8	−16.0	−21.2	61.8	−1555
	108°	−3.1(−4.3/−1.9)	−3.4	−12.1	−15.3	−15.2(−16.0/−14.3)	−21.7(−21.3/−22.1)	68.3 (70.1/66.5)	−1855
	36°	−2.0 (0.1/−4.2)	−3.8	−10.1	−15.4	−14.5(−15.1/−13.9)	−22.4(−22.8/−22.1)	62.8 (61.3/64.3)	−1647
Exptl[c]		*0.8*	*−2.6*	*−9.2*	*−12.3*	*−12.3*	*−17.9*	*56.4*	–
{*Exptl*[d]}		*−2.9*	*1.2*	*−9.2*	*−11.1*	*−11.8*	*−16.8*		

1,9s		B(2)	B(7)	B(8)	B(10)	B(4)	B(12)	B(11)	B(6)	B(5)	C(1)	C(9)	Co
	180°	2.8	1.1	−4.7	−7.7	−9.0	−14.4	−17.3	−21.5	−24.6	58.0	52.3	−2568
	108°	−0.8	3.6	−4.7	−8.4	−11.1	−13.8	−16.0	−21.7	−26.1	62.8	51.5	−2716
	36°	2.1	−0.5	−1.6	−7.9	−10.5	−12.6	−16.2	−23.0	−25.5	59.9	51.3	−2758

1,9a		B(2)	B(7)	B(8)	B(10)	B(4)	B(12)	B(11)	B(6)	B(5)	C(1)	C(9)	Co
	180°	2.6	0.0	−3.9	−7.6	−8.5	−14.3	−17.3	−22.0	−24.1	57.9	52.2	−2567
	108°	−0.4	3.0	−5.1	−8.4	−10.7	−13.8	−16.3	−21.3	−26.1	63.6	51.4	−2737
	36°	2.9	−0.7	−2.3	−7.9	−10.9	−12.8	−15.9	−22.6	−25.6	61.9	51.3	−2779
{*Exptl*[c]}		*0.4*	*−0.2*	*−1.9*	*−3.0*	*−8.3*	*−10.3*	*−12.7*	*−18.4*	*−19.9*			

1,12		B(5,6)	B(2,4)	B(10)	B(9,11)	B(5,6)	C(1)	C(12)	Co
	180°	−5.5	−6.4	−8.5	−20.7	−22.8	70.6	59.8	−2711
	108°	−4.3 (−2.9/−5.6)	−7.9 (−8.0/−7.8)	−8.5	−20.5(−21.3/−19.8)	−23.0(−24.2/−21.8)	74.2	61.6	−2815
	36°	−4.2 (−5.1/−3.3)	−7.1 (−6.5/−7.7)	−8.4	−20.6(−21.1/−20.1)	−23.6(−24.1/−23.1)	72.1	62.6	−2888
{*Exptl*[c]}		*−4.2*	*−6.4*	*−2.6*	*−16.1*	*−19.3*			

[a] Averaged under the assumption of rapid rotation, where applicable (in parentheses: values in static minima). [b] Cs^+ salt, from references. [46,56]. [c] From reference [56]. [c] This work. [d] Experimental data for $Co(C_5H_5)(x,y\text{-}C_2B_9H_{11})$ from ref. [38]; tentative assignments based on relative intensities and best accord with computed values.

Table 6. Chemical shifts [ppm] of the isomeric carboranes $C_2B_{10}H_{12}$ (GIAO-B3LYP/II′//BP86/AE1 level). In italics: experimental values.[a]

Isomer		Nuclei				
		C1,2	*B9,12*	*B8,10*	*B4,5,7,11*	*B3,6*
1,2	calcd	59.8	−3.0	−11.2	−16.4	−18.1
	exptl	*55.5*	*−3.1*	*−9.6*	*−13.7*	*−14.0*
		C1,7	*B5,12*	*B9,10*	*B4,6,8,11*	*B2,3*
1,7	calcd	61.4	−8.3	−12.3	−15.9	−20.2
	exptl	*55.1*	*−6.6*	*−10.4*	*−12.9*	*−16.3*
		C1,12	*B2–11*			
1,12	calcd	71.5	−17.4			
	exptl	*63.5*	*−15.2*			

[a] From reference [47].

metrical parameters can have a large impact on computed chemical shifts[7b]), we also evaluated the δ values using the experimental X-ray geometry. Since the positions of the protons are frequently ill-determined with the latter technique, we took just the coordinates of the non-hydrogen atoms from experiment[4a] and optimized the hydrogen positions at the BP86/AE1 level. The performance of such "H-relaxed" experimental geometries in energy and chemical-shift calculations has been used to assess the quality of these geometries.[8] For the H-relaxed X-ray and the fully optimized BP86 geometry of **1**, very similar $\delta(^{11}B)$ values are computed, within about 1 ppm of each other. The good mutual accord between (H-relaxed) experimental and optimized geometry of **1** is also illustrated by the fact that they differ by only 4 kJ mol^{-1} in energy (BP86/AE1 level). It is thus unlikely that the underlying DFT geometry is the source of the apparent problem with the theoretical $\delta(^{11}B)$ pattern of **1**.

To test whether this pattern is sensitive to the rotational dynamics, in particular to the population of individual rotamers in an equilibrium mixture, we computed the chemical shifts of the rotamers with $\theta \approx 36$ and 108° and included the results in Table 5. Due to the lower symmetry in these rotamers, all atoms in one carbollide moiety are inequivalent, and nine signals would be expected in the ^{11}B NMR spectrum. However, as the populations of each rotamer and its enantiomer (e.g., with $\theta \approx 108$ and −108°) are identical, and since interconversion between these enantiomers is rapid on the NMR timescale, the B(9)/B(12), B(4)/B(7), and B(5)/B(11) signals would appear pairwise averaged with double intensity and thus produce a spectrum with apparent C_{2h} (or C_{2v}) symmetry. These averaged spectra of the rotamers differ noticeably from that of C_{2h}-symmetric **1**, relative to which individual signals can change up to almost 4 ppm

(e.g., see B(8) for $\theta \approx 36°$ and 180° in Table 5).[50] This rotational dependence is illustrated in Figure 4.

In the rotamers with $\theta \approx 108$ and 36°, the B(9,12) and B(4,7) resonances are indeed shifted closer to each other (e.g., for $\theta \approx 36°$ they differ by merely 2.3 ppm, see Table 5), which would improve accord with experiment. However, deviations for other resonances are increased, so that the overall mean absolute error remains almost constant at around 3.2–3.3 ppm for all rotamers. The maximum deviation from experiment even increases from 4.1 ppm ($\theta = 180°$) to 5.1 and 5.8 ppm (B(6) for $\theta \approx 108$ and 36°, respectively). Even more striking is the wider spread of the signals, that is, the difference Δ between the most shielded and deshielded signals, B(6) and B(8), respectively, on rotation. For $\theta = 180°$, this spread ($\Delta = 29.9$ ppm) is in excellent accord with experiment ($\Delta = 29.2$ ppm for the Cs^+ salt), whereas much larger values are obtained for $\theta \approx 108$ and 36° ($\Delta = 35.6$ and 37.2 ppm, respectively). This increase in spread is clearly visible in the schematic sketches in Figure 4. Thus, the overall agreement with experiment is not improved over that achieved for C_{2h}-symmetric **1** when the predominance or partial population of other rotamers is assumed.

We also assessed the effect of the density functional employed in the NMR computations. The B3LYP functional was initially chosen because of its good performance for chemical shifts of transition-metal complexes, in particular for those of the metal nuclei themselves.[13a,b,14] For C_{2h}-symmetric **1** we tested some other popular functionals, such as LDA, PBE, and BHLYP (always employing the same BP86/AE1 geometry). As can be inferred from the results in Table 7 and Figure 5, little qualitative change in the $\delta(^{11}B)$ NMR pattern occurs on switching the functional. Only at the Hartree–Fock (HF) level, are completely unreliable results obtained, as expected, and the BHLYP functional, probably due to its large contribution of HF exchange, affords a slightly different ^{11}B NMR pattern. Even though for **1**, apparently, none of the functionals tested performs better than B3LYP, the general superiority of this functional for metallaboranes has yet to be established.

Table 7. Dependence of the computed chemical shifts [ppm] of **1** on the choice of density functional.[a]

Functional	B(8)	B(10)	B(4,7)	B(9,12)	B(5,11)	B(6)	C(1,2)	Co
HF[b]	−26.6	−17.3	−27.0	−7.4	−35.6	−40.6	−26.9	4106
PBE	3.2	−0.3	−5.2	−12.7	−23.3	−28.4	66.7	−1952
LDA	2.5	−0.6	−6.8	−14.8	−25.8	−31.6	73.0	−1872
BHLYP	0.8	−6.9	−5.7	−7.3	−22.8	−25.6	48.0	−1500
B3LYP	3.9	−2.4	−3.9	−9.5	−21.9	−26.0	61.1	−1843
Expt[c]	*5.8*	*0.9*	*−6.0*	*−6.6*	*−17.6*	*−23.0*	*51.9*	

[a] II′ basis, BP86/AE1 geometry. [b] Hartree–Fock data for comparison. [c] Cs^+ salt, this work.

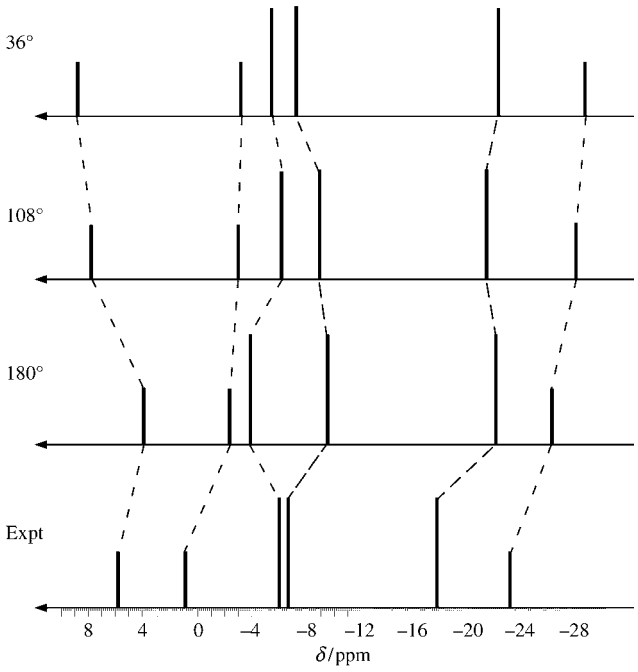

Figure 4. Schematic representations of experimental (bottom) and theoretical ^{11}B NMR spectra for **1** and its rotamers.

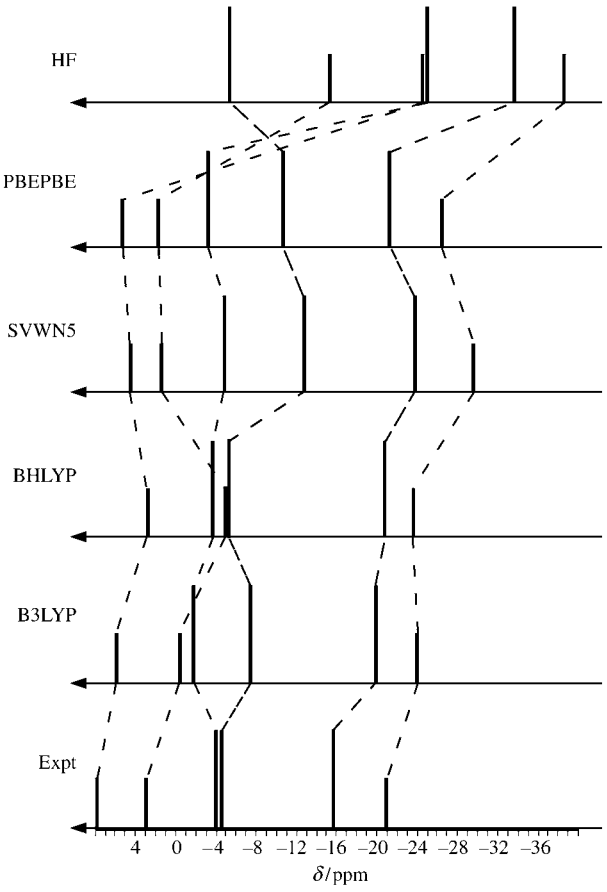

Figure 5. Schematic representations of experimental (bottom) and theoretical ^{11}B NMR spectra for **1**, computed with different density functionals.

Finally, we probed the sensitivity of the computed chemical shifts to a surrounding medium using a popular polarizable continuum model (PCM)[51] and employing the dielectric constant of the solvent used in the experiments, acetone.[46] Occasionally, notable such "direct" solvation effects on chemical shifts (i.e., through the response of the electronic wavefunction) can be found.[52] More often, however, such direct effects are small and can be superseded by "indirect" effects, that is, by changes in the molecular geometry on solvation.[53] These latter effects (which could be modeled by optimizing the geometry in the presence of a continuum) are expected to be small for **1**, given the slight sensitivity of the computed $\delta(^{11}B)$ values toward the details of the geometrical parameters (see above). Thus, a single-point PCM calculation was performed for the gas-phase BP86/AE1 geometry. On going from the vacuum into the continuum, no qualitative and only minor quantitative changes in the ^{11}B chemical shifts (up to ca. 1.5 ppm) occurred. Likewise, counterion effects should be small,[54] so that the values computed for the pristine ion in the gas phase (as discussed in the preceding part) should be comparable to experiments in solution.

Even though the 1,7 isomer of **1** has been known for a long time,[35] no ^{11}B NMR data seem to have been reported yet. We have now (re)determined the ^{11}B and ^{13}C chemical shifts of this species, which are included with the computed values in Table 5. The degree of agreement between theory and experiment is very good, and the mean and maximum absolute deviations of 2.4 and 3.7 ppm, respectively (for the 180° isomer) are similar to those found for **1**.

Table 5 also contains the predicted δ values for the 1,9 and 1,12 isomers, which are the most stable according to the energetics in Table 2. These data may be compared to experimental values obtained for the corresponding, related Co(C_5H_5)($C_2B_9H_{11}$) isomers,[38] which are included in Table 5. Assuming no significant changes in $\delta(^{11}B)$ between the mono- and bis-dicarbollide species (which is borne out by the data for the 1,2 and 1,7 forms), it appears that the ^{11}B chemical shifts are described with a similar accuracy for **1** and its isomers, with a slightly larger maximum deviation of about 6 ppm for the latter (see B(10) in the 1,12 isomer, Table 5). The deviations are not systematic in all cases, so that the relative ordering of close-lying signals can differ between theory and experiment (e.g., for B(2,4) and B(10) in the 1,12-form, Table 5).

In summary, the experimental ^{11}B chemical shifts of **1** are qualitatively well reproduced at the GIAO-B3LYP/II′//BP86/AE1 level. At this and other DFT levels, a somewhat lower quantitative accuracy is obtained, as compared to earlier ab initio data on boranes and carboranes, and errors as large as about 5 ppm can occur. These errors are not remedied by allowing for changes in geometrical parameters (bond lengths, dihedral angles) or inclusion of solvation effects, and appear to be inherent to the density functionals employed. Further development of new functionals and assessment of their performance in NMR computations is thus warranted.

^{13}C: The ^{13}C chemical shifts, included in Tables 5 and 6, are rather unremarkable. For the 1,2- and 1,7-carboranes, as well as for C_{2h}-symmetric **1** and its 1,7-isomer, very similar $\delta(^{13}C)$ values around 60 ppm are computed. While these data are in reasonable agreement with experiment for the carboranes,[55] with a largest deviation of 8 ppm for 1,12-$C_2B_{10}H_{12}$ (Table 6), a somewhat larger error of more than 10 ppm is found for **1**.[56] More metallacarboranes should be computed to test whether such errors are common and, possibly, systematic. A somewhat smaller error of about 5 ppm is found for the 1,7 isomer of **1** (Table 5). As with the ^{11}B shifts discussed above, only minor changes in $\delta(^{13}C)$ are introduced by employing the H-relaxed X-ray geometries, other rotamers, other density functionals, or a polarizable continuum.

^{59}Co: Among the transition metals, ^{59}Co is a relatively well-behaved NMR nucleus,[57] which can be observed in a wide variety of compounds, including fairly large biomolecules such as vitamin B_{12}.[58] In metallacarboranes such as **1**, the presence of quadrupolar boron nuclei adjacent to ^{59}Co may render the observation of the latter nucleus difficult, if not impossible. To our knowledge, no ^{59}Co NMR data have been reported for any cobaltaborane to date. Such data would be desirable, as NMR spectroscopy of the metal center can be a valuable probe for structures and reactivities of transition-metal complexes.[59] We therefore report predictions for the $\delta(^{59}Co)$ values of **1** and its isomers, to provide some guidance for eventual detection. For a number of inorganic and organometallic Co compounds, the ^{59}Co chemical shifts (which cover a total range of ca. 20000 ppm) have been well reproduced by suitable DFT methods,[13b,c,g] including the B3LYP/II′//BP86/AE1 level employed here.[13g]

At this level, $\delta(^{59}Co) = -1843$ ppm is predicted for pristine C_{2h}-symmetric **1** (Table 5), that is, shielded by 567 ppm with respect to the cobalticenium ion $[Co(C_5H_5)_2]^+$, with $\delta(^{59}Co) = -2410 \pm 25$ ppm.[28]

Geometrical changes affect the computed ^{59}Co chemical shift much more than $\delta(^{11}B)$ or $\delta(^{13}C)$, consistent with the much larger shift range of the metal. In the H-relaxed X-ray geometry of **1**, the ^{59}Co nucleus is shielded by about 200 ppm relative to that in the fully optimized BP86 geometry. Likewise, in the rotamers with $\theta \approx 108$ and 36°, the metal is shielded relative to the C_{2h} form by about 75 and 200 ppm, respectively. A slight deshielding, by less than 20 ppm, results from the PCM calculation. The dramatic effect of the particular density functional employed on transition-metal chemical shifts in general,[14] and on $\delta(^{59}Co)$ in particular,[13b,c] has been noted before. The superiority of hybrid functionals such as B3LYP is well established in this case, and we will refrain from discussion of results obtained with other functionals (which are inlcuded in Table 7). We will also not go into zero-point and classical thermal corrections, which, according to suitable approaches based on perturbation theory and molecular dynamics simulations,[13g,h] can be quite sizeable for $\delta(^{59}Co)$, for which they can amount to several hundreds of ppm.[13h] Corresponding simulations

for **1** would be a formidable task, beyond the scope of the present paper.[60]

Taking into account all uncertainties in the theoretical δ(^{59}Co) value of **1** that arise from the deficiencies of the methodology applied,[13h] and from possible effects of rotational (and molecular) dynamics, an error margin of 500–600 ppm would seem conservative. We are confident that the ^{59}Co chemical shift of **1**, if it is ever be recorded, will be found in the region between −1800 and −2400 ppm. Such an error margin may seem large at first sight, but it should be kept in mind that this is just a few percent of the total ^{59}Co chemical shift range.

For the 1,7-isomer of **1**, $\delta(^{59}\text{Co}) = -1555$ ppm is computed (Table 5), that is, 288 ppm less shielded than in **1**, which would correspond, with the same primary reference and error margin, to a predicted range between −1500 and −2100 ppm. Increased shielding of the ^{59}Co nucleus is computed for the other isomers that have only one carbon atom of each carbollide moiety attached to the metal (1,5, 1,9, 1,10, and 1,12 isomers), with δ values between −1918 and −2888 ppm. Even more shielded $\delta(^{59}\text{Co})$ values, between −2879 and −3566 ppm, are obtained for forms that have only B atoms as nearest neighbors of cobalt (5,6, 5,11, and 5,10 isomers, not included in Table 5). ^{59}Co NMR spectroscopy of cobaltaboranes could thus be a very sensitive analytical probe for the coordination sphere about the metal atom.

Conclusion

We have presented the first computational characterization of the cobalt bis(dicarbollide) ion [3-Co-(1,2-$C_2B_9H_{11})_2$]$^-$ (**1**) using the modern tools of density functional theory. The BP86/AE1 potential energy surface of **1** is characterized by three different rotamers with staggered conformation of the two dicarbollide moieties. These minima are separated by three distinct eclipsed transition states. The minima are close in energy and the barriers between them are low (less than 37 kJ mol^{-1}), consistent with facile rotation about the long molecular axis. In keeping with empirical stability rules, **1** is not the most stable form, and other positional isomers with nonadjacent carbon atoms are found to be lower in energy. As most stable form we identified the 1,7 isomer [2-Co-(1,7-$C_2B_9H_{11})_2$]$^-$, which has also been isolated and which is probably the global minimum, 121 kJ mol^{-1} lower in energy than **1**.

The observed ^{11}B chemical shifts of **1** and its 1,7 isomer can be reproduced with an accuracy of about 3–5 ppm at the GIAO-B3LYP/II′level. The computed $\delta(^{11}\text{B})$ values are little affected (on the order of only 1 ppm) by rotational mobility or by embedding the pristine ions in a polarizable continuum. A similar accuracy was found for the metal-free carboranes $C_2B_{10}H_{12}$. As far as ^{11}B chemical shifts of heteroboranes are concerned, the performance of conventional ab initio methods is somewhat better than that of the density-functional approaches employed in this study. Apparently, however, the quality of the DFT-based $\delta(^{11}\text{B})$ values does not degrade in the presence of a transition metal. This finding, together with the qualitatively reasonable description of ^{11}B chemical shifts at that level, suggests that the huge family of transition-metal-containing heteroboranes should be amenable to ^{11}B NMR computations and applications thereof. The point appears within reach, at which structural assignments and refinements of such metallaheteroboranes can be aided by chemical-shift calculations, in much the same way as it is now routinely being done for metal-free heteroboranes. Given that properties of transition-metal compounds can pose severe problems for many theoretical methods, this broadened array of targets for NMR applications represents not only a gain in quantity, but also in quality. Further validation studies along these lines, comprising a larger set of transition metals, are in progress.

A ^{59}Co chemical shift between −1800 and −2400 ppm is predicted for **1**, close to that of the cobalticenium ion with its related electronic structure. Experimental verification of this prediction will certainly be a challenge, but efforts in that direction may be rewarding: According to our computations, ^{59}Co NMR should be a very sensitive probe for the geometrical and electronic structure of **1** and its isomers, and, possibly, for the large family of other cobaltaboranes.

Acknowledgements

This work was supported by the German Academic Exchange Service (DAAD) and the Academy of Sciences of the Czech Republic in the joint PPP programme, as well as the Ministry of Education of the Czech Republic (project no. LC523).. M.B. thanks the Deutsche Forschungsgemeinschaft for a Heisenberg fellowship and Prof. W. Thiel for continuous support.

[1] See for instance: I. B. Sivaev, V. I. Bregadze, *J. Organomet. Chem.* **2000**, *614*, 27 and references therein.
[2] a) M. F. Hawthorne, D. C. Young, P. A. Wegner, *J. Am. Chem. Soc.* **1965**, *87*, 1818; b) M. F. Hawthorne, T. D. Andrews, *J. Chem. Soc. Chem. Commun.* **1965**, 443.
[3] For example: I. B. Sivaev, V. I. Bregadze, *Collect. Czech. Chem. Commun.* **1999**, *64*, 783.
[4] For selected examples (with reference code from the Cambridge Structure Database), see a) QAJNAQ: M. J. Hardie, C. L. Raston, *Angew. Chem.* **2000**, *112*, 3993; *Angew. Chem. Int. Ed.* **2000**, *39*, 3835; b) RINMIK: R. M. Chamberlin, B. L. Scott, M. M. Melo, K. D. Abney, *Inorg. Chem.* **1997**, *36*, 809; c) WEZHOY: X. Zuowei, T. Jelínek, R. Bau, C. A. Reed, *J. Am. Chem. Soc.* **1994**, *116*, 1907; d) BEVBUZ: L. Borodinsky, E. Sinn, R. N. Grimes, *Inorg. Chem.* **1982**, *21*, 1686.
[5] The electronic structure has been studied at lower levels of theory; for a recent study including HF/3-21G results, see I. Rojo, F. Teixidor, C. Vinas, R. Kivekäs, R. Sillanpää, *Chem. Eur. J.* **2003**, *9*, 4311.
[6] J. Plešek, *Chem. Rev.* **1992**, *92*, 269, and references therein.
[7] a) M. Bühl, P. von R. Schleyer, *J. Am. Chem. Soc.* **1992**, *114*, 477; b) Review: M. Bühl in *Encyclopedia of Computational Chemistry* (Eds.: P. von R. Schleyer, N. L. Allinger, P. A. Kollman, T. Clark, H. F. Schaefer, J. Gasteiger, P. R. Schreiner P. R.), Wiley, Chichester, **1998**, pp. 1835.
[8] Selected examples: a) D. Hnyk, E. Vajda, M. Bühl, P. von R. Schleyer, *Inorg. Chem.* **1992**, *31*, 2464; b) D. Hnyk, M. Bühl, P. von R. Schleyer, H. V. Volden, S. Gundersen, J. Müller, P. Paetzold, *Inorg.*

Chem. **1993**, *32*, 2442; c) P. T. Brain, D. Hnyk, D. W. H. Rankin, M. Bühl, P. von R. Schleyer, *Polyhedron* **1994**, *13*, 1453; d) D. Hnyk, M. Hoffmann, P. von R. Schleyer, M. Bühl, D. W. H. Rankin, *J. Phys. Chem.* **1996**, *100*, 3434; e) P. T. Brain, M. Bühl, M. A. Fox, R. Greatrex, D. Hnyk, A. Nikrahi, D. W. H. Rankin, H. E. Robertson, *J. Mol. Struct.* **1998**, *445*, 319.

[9] The most recent examples include a) T. Jelínek, B. Štíbr, J. Holub, M. Bakardjiev, D. Hnyk, D. L. Ormsby, C. A. Kilner, M. Thornton-Pett, H.-J. Schanz, B. Wrackmeyer, B, J. D. Kennedy, *Chem. Commun.* **2001**, 1756; b) B. Štíbr, O. L. Tok, W. Milius, M. Bakardjiev, J. Holub, D. Hnyk, B. Wrackmeyer, *Angew. Chem. Int. Ed.* **2002**, *114*, 2230; *Angew. Chem. Int. Ed.* **2002**, *41*, 2126; c) T. Jelínek, B. Štíbr, J. D. Kennedy, D. Hnyk, M. Bühl, M. Hofmann, *Dalton Trans.* **2003**, 1326.

[10] T. Onak, J. Tseng, M. Diaz, D. Tran, J. Arias, S. Herrera, D. Brown, *Inorg. Chem.* **1993**, *32*, 487.

[11] a) S. Berger, W. Bock, G. Frenking, V. Jonas, F. Müller, *J. Am. Chem. Soc.* **1995**, *117*, 3820; b) M. Bühl, G. Hopp, W. von Philipsborn, S. Beck, M. Prosenc, U. Rief, H.-H. Brintzinger, *Organometallics* **1996**, *15*, 778; c) P. T. Brain, M. Bühl, J. Cowie, Z. G. Lewis, A. J. Welch, *J. Chem. Soc. Dalton Trans.* **1996**, 231.

[12] For examples of ligand chemical shifts, see a) M. Kaupp, V. G. Malkin, O. L. Malkina, D. R. Salahub, *Chem. Phys. Lett.* **1995**, *235*, 382; b) M. Kaupp, V. G. Malkin, O. L. Malkina, D. R. Salahub, *J. Am. Chem. Soc.* **1995**, *117*, 1851; c) Y. Ruiz-Morales, G. Schreckenbach, T Ziegler, *J. Phys. Chem.* **1996**, *100*, 3359; d) Y. Ruiz-Morales, G. Schreckenbach, T Ziegler, *Organometallics* **1996**, *15*, 3920.

[13] For metal shifts, see for example: a) M. Bühl, *Chem. Phys. Lett.* **1997**, *267*, 251; b) Godbout, Oldfield, *J. Am. Chem. Soc.* **1997**, *119*, 8065; c) J. C. C. Chan, S. C. F. Au-Yeung, *J. Phys. Chem.* **1997**, *101*, 3637; d) G. Schreckenbach, T. Ziegler, *Int. J. Quantum Chem.* **1997**, *61*, 899; e) M. Bühl, M. Parrinello, *Chem. Eur. J.* **2001**, *7*, 4487; f) A. Bagno, M. Bonchio, *Magn. Reson. Chem.* **2004**, *42*, S79; g) S. Grigoleit, M. Bühl, *Chem. Eur. J.* **2004**, *10*, 5541; h) S. Grigoleit, M. Bühl, *J. Chem. Theory Comput.* **2005**, *1*, 181.

[14] Reviews: a) M. Kaupp, V. G. Malkin, O. L. Malkina in *The Encyclopedia of Computational Chemistry* (Eds.: P. von R. Schleyer, N. L. Allinger, T. Clark, J. Gasteiger, P. A. Kollman, H. F. Schaefer III, P. R. Schreiner), Wiley, Chichester, **1998**, pp. 1857; b) G. Schreckenbach, T. Ziegler, *Theor. Chem. Acc.* **1998**, *99*, 71; c) M. Bühl in *Calculation of NMR and ESR Parameters. Theory and Applications* (Eds.: M. Kaupp, M. Bühl, V. G. Malkin) Wiley-VCH, Weinheim, **2004**, pp. 421.

[15] A. D. Becke, *Phys. Rev. A* **1988**, *38*, 3098.

[16] J. P. Perdew, *Phys. Rev. B* **1986**, *33*, 8822; J. P. Perdew, *Phys. Rev. B* **1986**, *34*, 7406.

[17] a) A. J. H. Wachters, *J. Chem. Phys.* **1970**, *52*, 1033; b) P. J. Hay, *J. Chem. Phys.* **1977**, *66*, 4377.

[18] a) W. J. Hehre, R. Ditchfield, J. A. Pople, *J. Chem. Phys.* **1972**, *56*, 2257; b) P. C. Hariharan, J. A. Pople, *Theor. Chim. Acta* **1973**, *28*, 213.

[19] See for instance: a) W. Koch, M. C. Holthausen, *A Chemist's Guide to Density Functional Theory*, Wiley-VCH, Weinheim, **2000**, and the extensive bibliography therein. Note that hybrid functionals such as B3LYP need not be superior to pure, gradient-corrected functionals as far as geometries of transition metal complexes are concerned; see, for example: b) C. J. Barden, J. C. Rienstra-Kiracofe, H. F. Schaefer, *J. Chem. Phys.* **2000**, *113*, 690; c) M. Bühl, S. Grigoleit, *Organometallics*, **2005**, *24*, 1516.

[20] A. E. Reed, L. A. Curtiss, F. Weinhold, *Chem. Rev.* **1988**, *88*, 899.

[21] R. F. W. Bader, *Atoms in Molecules*, Oxford Press, New York, **1990**.

[22] a) R. Ditchfield, *Mol. Phys.* **1974**, *27*, 789; b) K. Wolinski, J. F. Hinton, P. Pulay, *J. Am. Chem. Soc.* **1990**, *112*, 8251; c) GIAO-DFT implementation: J. R. Cheeseman, G. W. Trucks, T. A. Keith, M. J. Frisch, *J. Chem. Phys.* **1996**, *104*, 5497.

[23] A. D. Becke *J. Chem. Phys.* **1993**, *98*, 5648.

[24] C. Lee, W. Yang, R. G. Parr, *Phys. Rev. B* **1988**, *37*, 785.

[25] W. Kutzelnigg, U. Fleischer, M. Schindler in *NMR Basic Principles and Progress*, *Vol. 23*, Springer-Verlag, Berlin, **1990**, pp. 165–262.

[26] a) R. Bauernschmitt, R. Ahlrichs, *Chem. Phys. Lett.* **1996**, *256*, 454; b) R. E. Stratmann, G. E. Scuseria, M. J. Frisch, *J. Chem. Phys.* **1998**, *109*, 8218.

[27] T. P. Onak, H. L. Landesman, R. E. Williams, I. Shapiro, *J. Phys. Chem.* **1959**, *63*, 1533.

[28] E. A. C. Lucken, K. Noack, D. F. Williams, *J. Chem. Soc. A* **1967**, 148.

[29] S. H. Vosko, L. Wilk, M. Nusair, *Can. J. Phys.* **1980**, *58*, 1200.

[30] a) J. J. P. Perdew, K. Burke, M. Ernzerhof, *Phys. Rev. Lett.* **1996**, *77*, 3865; b) J. J. P. Perdew, K. Burke, M. Ernzerhof, *Phys. Rev. Lett.* **1997**, *78*, 1396.

[31] cf. A. D. Becke, *J. Chem. Phys.* **1993**, *98*, 1372.

[32] Gaussian 03 (Revision BO.1), M. J. Frisch, G. W. Trucks, H. B. Schlegel, G. E. Scuseria, M. A. Robb, J. R. Cheeseman, J. A. Montgomery, Jr., T. Vreven, K. N. Kudin, J. C. Burant, J. M. Millam, S. S. Iyengar, J. Tomasi, V. Barone, B. Mennucci, M. Cossi, G. Scalmani, N. Rega, G. A. Petersson, H. Nakatsuji, M. Hada, M. Ehara, K. Toyota, R. Fukuda, J. Hasegawa, M. Ishida, T. Nakajima, Y. Honda, O. Kitao, H. Nakai, M. Klene, X. Li, J. E. Knox, H. P. Hratchian, J. B. Cross, C. Adamo, J. Jaramillo, R. Gomperts, R. E. Stratmann, O. Yazyev, A. J. Austin, R. Cammi, C. Pomelli, J. W. Ochterski, P. Y. Ayala, K. Morokuma, G. A. Voth, P. Salvador, J. J. Dannenberg, V. G. Zakrzewski, S. Dapprich, A. D. Daniels, M. C. Strain, O. Farkas, D. K. Malick, A. D. Rabuck, K. Raghavachari, J. B. Foresman, J. V. Ortiz, Q. Cui, A. G. Baboul, S. Clifford, J. Cioslowski, B. B. Stefanov, G. Liu, A. Liashenko, P. Piskorz, I. Komaromi, R. L. Martin, D. J. Fox, T. Keith, M. A. Al-Laham, C. Y. Peng, A. Nanayakkara, M. Challacombe, P. M. W. Gill, B. Johnson, W. Chen, M. W. Wong, C. Gonzalez, and J. A. Pople, Gaussian, Inc., Pittsburgh PA, **2003**.

[33] P. L. A. Popelier, *Comput. Phys. Commun.* **1996**, *93*, 212.

[34] Electrostatic arguments, specifically the induction energy of the metal in the potential field of the rings, have been put forward to rationalize the preference of the eclipsed over the staggered form of ferrocene: S. Carter, J. N. Murrell, *J. Organomet. Chem.* **1980**, *192*, 399.

[35] M. F. Hawthorne, D. C. Young, T. D. Andrews, D. V. Howe, R. L. Pilling, A. D. Pitts, M. Reintjes, L. F. Warren, Jr., P. A. Wegener, *J. Am. Chem. Soc.* **1968**, *90*, 879.

[36] a) *C*-Ph derivative: C. Viñas, S. Gomez, J. Bertran, J. Barron, F. Teixidor, J.-F. Dozol, H. Rouquette, R. Kivekäs, R. Sillanpää, *J. Organomet. Chem*. **1999**, 581, 188; b) neutral *B*-PMe_3 derivative: A. Franken, J. Plešek, J. Fusek, M. Semrau, *Collect. Czech. Chem. Commun.* **1997**, *62*, 1070.

[37] a) B,C′ bridged derivative with 1,2- and 1,9-C_2B_9 cores: C. Viñas, J. Pedrajas, F. Teixidor, R. Kivekäs, R. Sillanpää, A. J. Welch, *Inorg. Chem.* **1997**, *36*, 2988; b) [1,11-Ph_2-3-Co(1,11-$C_2B_9H_9$)(pyridine)]: J. Bertran, C. Viñas, S. Gomez, M. Lamrani, F. Teixidor, R. Sillanpää, R. Kivekäs, *Collect. Czech. Chem. Commun.* **1997**, *62*, 1263.

[38] M. K. Kaloustian, R. J. Wiersema, M. F. Hawthorne, *J. Am. Chem. Soc.* **1972**, *94*, 6679.

[39] Such rearrangements are also known for other metallacarboranes, L. F. Warren, Jr., M. F. Hawthorne, *J. Am. Chem. Soc.* **1970**, *92*, 1157.

[40] a) R. E. Williams, F. J. Gerhart, *J. Am. Chem. Soc.* **1965**, *87*, 3513; b) K. Wade, *Adv. Inorg. Chem. Radiochem.* **1976**, *18*, 1; c) R. E. Williams, *Adv. Inorg. Chem. Radiochem.* **1976**, *18*, 67.

[41] a) M. Hofmann, M. A. Fox, R. Greatrex, P. von R. Schleyer, R. E. Williams, *Inorg. Chem.* **2001**, *40*, 1790; b) F. A. Kiani, M. Hofmann, *Inorg. Chem.* **2004**, *43*, 8561.

[42] See also: D. A. Brown, M. O. Fanning, N. J. Fitzpatrick, *Inorg. Chem.* **1978**, *17*, 1620.

[43] K. Wiberg, *Tetrahedron* **1968**, *24*, 1083.

[44] See for example: a) S. J. A. van Gisbergen, J. A. Groeneveld, A. Rosa, J. G. Snijders, E. J. Baerends, *J. Phys. Chem. A* **1999**, *103*, 6835; b) C. Adamo, V. Barone, *Theor. Chem. Acc.* **2000**, *105*, 169; c) A. Rosa, G. Ricciardi, O. Gritsenko, E. J. Baerends in *Structure and Bonding*, *Vol. 112* (Eds.: N. Kaltsoyannis, J. E. McGrady), Springer, Berlin, Heidelberg, **2004**, pp. 49.

[45] L. Mátel, F. Macášek, P. Rajec, S. Heřmánek, J. Plešek, *Polyhedron* **1982**, *1*, 511.
[46] [D_6]Acetone solution: a) A. N. Gashti, J. C. Huffman, A. Edwards, G. Szekeley, A. R. Siedle, J. A. Karty, J. P. Reilly, L. J. Todd, *J. Organomet. Chem.* **2000**, *614*, 120 (Na^+ counterion); b) I. Rojo, F. Teixidor, R. Kivekäs, R. Sillanpää, C. Viñas, *Organometallics* **2003**, *22*, 4642 (Cs^+ counterion); c) CD_3CN solution (Cs^+ counterion): this work.
[47] ^{11}B data from a) F. P. Boer, R. A. Hegstrom, M. D. Newton, J. A. Potenza, W. N. Lipscomb, *J. Am. Chem. Soc.* **1966**, *88*, 5340; A. R. Garber, G, . M. Bodner, L. J. Todd, *J. Magn. Reson.* **1977**, *28*, 383; b) ^{13}C data from: c) M. Diaz, J. Jaballas, J. Arias, H. Lee, T. Onak, *J. Am. Chem. Soc.* **1996**, *118*, 4405.
[48] As is usually the case with complexes of middle and late transition metals, very poor chemical shifts are obtained for **1** at the Hartree–Fock level.
[49] We did not make such an adjustment from the onset, because this would be difficult to generalize for other metallaboranes with varying carbon content.
[50] As with C_{2h}-symmetric **1**, the H-relaxed X-ray and fully optimized BP86 geometries of the rotamer with $\theta \approx 36°$ are very close in energy (within 3 kJ mol^{-1} at BP86/AE1) and afford very similar δ(^{11}B) values.
[51] a) V. Barone, M. Cossi, J. Tomasi *J. Comput. Chem.* **1998**, *19*, 404; b) M. Cossi, G. Scalmani, N. Rega, V. Barone, *J. Chem. Phys.* **2002**, *117*, 43; c) M. Cossi, O. Crescenzi, *J. Chem. Phys.* **2003**, *119*, 8863.
[52] For a recent application to δ(^{15}N) in nitroimidazoles, see T. C. Ramalho, M. Bühl, *Magn. Reson. Chem.* **2005**, *43*, 139.
[53] For example, $BH_3{\cdot}NH_3$: M. Bühl, T. Steinke, P. von R. Schleyer, R. Boese, *Angew. Chem.* **1991**, *103*, 1179; *Angew. Chem. Int. Ed. Engl.* **1991**, *30*, 1160.
[54] For example, the computed ^{11}B chemical shift of $B_3H_8^-$ changes very little on complexation with Li^+ or Na^+, cf. ref. [7a].
[55] The same has been found previously.[7a,47b] See also J. M. Oliva, C. Viñas, *J. Mol. Struct.* **2000**, *556*, 33.
[56] ^{13}C data for **1** from: A. R. Siedle, G. M. Bodner, A. R. Garber, D. C. Beer, L. J. Todd, *Inorg. Chem.* **1974**, *13*, 2321.
[57] P. S. Pregosin in *Transition Metal Nuclear Magnetic Resonance*, (Ed.: P. S. Pregosin), Elsevier, Amsterdam, **1991**, pp. 144.
[58] For example: A. Medek, V. Frydman, L. Frydman, *Proc. Natl. Acad. Sci. USA* **1997**, *94*, 14237.
[59] W. von Philipsborn, *Chem. Soc. Rev.* **1999**, *28*, 95.
[60] By using the experimental geometry from the solid state, as discussed above in the text, effects of vibrational averaging from the cages are to some extent accounted for. A referee suggested to provide an estimate of the rovibrational corrections from the C–H and B–H bonds (which are missing in the H-relaxed geometries). We performed additional calculations for **1** with each of the X–H bonds elongated by 0.01 Å (explicit calculation of the vibrationally averaged geometry of B_2H_6 affords an elongation of the terminal B–H bonds by 0.006 Å at the BP86/6-31G* level); only minor, non-site-specific changes in the shielding constants of the heavier nuclei occurred, which did not exceed 0.3 and 3 ppm for ^{11}B and ^{59}Co, respectively.

Received: November 24, 2004
Published online: April 29, 2005